

Analysis of wettability and oil-water separation mechanism of superhydrophilic/underwater superoleophobic mesh based on capillary force model

Yuanfeng Fu, Zhenzhong Fan*, Qingwang Liu, Qilei Tong, Li Cai

The Key Laboratory of Enhanced Oil and Gas Recovery, Ministry of Education, Northeast Petroleum University, Daqing, 163318, China

*fanzhenzhong@nepu.edu.cn

Abstract. The Frequent oil spills at sea and large discharges of oily wastewater spills seriously jeopardize the ecological environment and lead to an increasing shortage of water resources, so the oil/water separation has become a hot spot of global research. As opposed to the conventional separation method, the membrane separation has received wide attention because of its advantages of green environmental protection, low energy consumption and easy operation. In this paper, $\text{Cu}(\text{OH})_2$ mesh with superhydrophilic and underwater superoleophobic properties were prepared by in-situ growth method using purple copper mesh as the substrate. Scanning electron microscopy, x-ray photoelectron spectroscopy and contact angle tests were used to evaluate the surface morphology, chemical composition and wetting behavior of the mesh. The results showed that the water contact angle was 0° in air and the contact angle was 155.4° for oil droplets underwater. The membrane exhibited high separation efficiencies (99%) and separation fluxes ($3.67\text{--}6.54 \times 10^4 \text{ L} \cdot \text{m}^{-2} \cdot \text{h}^{-1}$) for the five tested oils under gravity drive. The wettability of the mesh was unaffected after 20 separation experiments. The surface wettability and the oil/water separation mechanism were analyzed using the capillary force-based separation model combined with the Young and Cassie-Baxter equations.

Keywords: membrane; wettability; oil/water separation; superhydrophilic; capillary force

1. Introduction

Although industrialization has accelerated the development of human civilization, it has also over-consumed natural resources at an unsustainable rate and brought about severe ecological pollution problems, such as oily wastewater produced in the process of petroleum development, transportation, and processing, which not only aggravates the shortage of water resources but also affects the ecological balance of the water [1]. In recent years, the membrane separation method has shown great application value in treating oily wastewater. Compared with traditional treatment methods, such as gravity separation, chemical flocculation, biological treatment, and electro-condensation, this method has the advantages of a small footprint, green energy-saving, and easy to operate, which is considered to be one of the most effective methods for treating oily wastewater [2]. For oil/water separation membranes, the most important thing is to construct a super wetted surface. Inspired by the extraordinary wetting phenomenon in nature [3], the preparation of bionic artificial super-wettable surfaces has been rapidly developed, which has a bright application prospect in oily wastewater treatment. It is mainly due to the advantages of adjustable selectivity, high separation efficiency and reusability [4]. The construction of superwettability membrane materials is related to the microscopic roughness structure and surface energy [5]. Currently, according to the difference in wettability is categorized into superhydrophobic-superoleophilic membranes and superhydrophilic-underwater superoleophobic membranes [6]. Compared with the disadvantages of superhydrophobic membranes, which are easily contaminated and clogged by oil and have a short service life, superhydrophilic-underwater superoleophobic membranes have better anti-pollution and recycling capabilities [7]. Xue et al. coated hydrophilic polyacrylamide hydrogel on stainless steel mesh. The underwater oil droplet contact angle reached $155.3^\circ \pm 1.8^\circ$, with a separation efficiency of 99% [8]. Gao et al. prepared a dual-scaled porous nitrocellulose membrane

using a simple perforation method. The underwater oil droplet contact angle was $156.4^{\circ} \pm 3.2^{\circ}$ and separation efficiency was more than 99% [9].

In this paper, the superhydrophilic/underwater superoleophobic $\text{Cu}(\text{OH})_2$ mesh was prepared by constructing micro and nanoscale three-dimensional rough structures on the surface of copper mesh, with a water contact angle of 0° in air and a contact angle of 155.4° for oil droplets underwater. The separation efficiency of the five types of oil/water mixtures was higher than 99%, and the surface wettability was not affected after 20 times oil/water separation experiments. The separation mechanism of oil/water mixtures is mainly based on the size-sieving principle of special wetted surfaces. Still, there is no unified explanation method for analysing the mechanism. Herein, we used the Capillary force-based separation (CFS) model in combination with the Young and the Cassie-Baxter equations to explain the surface wettability and oil/water separation mechanism.

2. Experimental

2.1 Materials

Copper mesh (CM, 250 mesh size) was purchased from Saichi Metal Wire Products Co., Ltd, China. Sodium hydroxide (NaOH, 95%), potassium persulfate ($\text{K}_2\text{S}_2\text{O}_8$, 99.5%), methylene blue and oil red O were obtained from Macklin Biochemical Technology Co., Ltd, China. Hydrochloric acid (HCl, 36%), anhydrous ethanol (EtOH, 99.7%) were obtained from Sinopharm Chemical Reagent Co., Ltd, China. All the chemicals were used as received without any further purification.

2.2 Fabrication of $\text{Cu}(\text{OH})_2$ -CM

The copper mesh (30mm \times 30mm) was immersed in 1M HCl, anhydrous ethanol sonication for 15 minutes to remove the oxide layer on the surface. After washing with distilled water three times and then drying naturally at room temperature, the cleaned copper mesh did not have other atomic impurities to affect the experimental results, which was marked as CM.

Preparation of solution A: The $\text{K}_2\text{S}_2\text{O}_8$ (2.7032 g) was dissolved in 100 mL distilled water (2.5×10^{-4} M). Preparation of solution B: The NaOH (8.0 g) was dissolved in 100 mL distilled water (5×10^{-3} M). Then, the two solutions were mixed and stirred for 5 minutes until clarified. The CM was placed in the mixed solution for 30 minutes at 298 K. Finally the mesh was washed with distilled water and dried at room temperature to obtain the $\text{Cu}(\text{OH})_2$ -CM. The schematic illustration of the preparation processes is shown in Fig. 1.

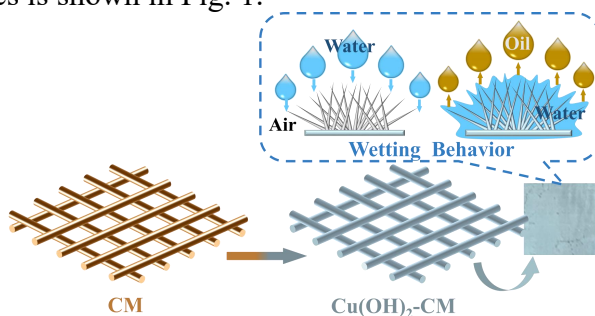


Fig. 1. Schematic illustration of the preparation processes of the $\text{Cu}(\text{OH})_2$ -CM

2.3 Oil/water separation experiments

A homemade oil/water separation unit measured separation efficiency (R) and membrane flux (F). The mixture of water and oil (hexane, kerosene, xylene, diesel and gasoline) was mixed in a 1:1 mass ratio. The test oil was stained with oil red O and the water with methylene blue for precise observation. Before the oil/water separation experiments, the $\text{Cu}(\text{OH})_2$ -CM was pre-wetted with water. The oil/water separation experiments were performed only under the effect of gravity. The separation efficiency can be calculated according to equation (1):

$$R = M/M_0 \times 100\% \quad (1)$$

where R represents the separation efficiency and M and M_0 represent the mass of water before and after filtration.

The membrane flux (F) can be calculated according to equation (2):

$$F = V / A \times t \quad (2)$$

where F ($\text{L} \cdot \text{m}^{-2} \cdot \text{h}^{-1}$) is the membrane flux, V (L) is the volume of filtered water, A (m^2) is the effective membrane area, $1.26 \times 10^{-3} \text{ m}^2$, and t (h) is the separation time.

2.4 Characterization

The surface micromorphology of CM, $\text{Cu}(\text{OH})_2\text{-CM}$ was observed by scanning electron microscopy (SEM, Zeiss Gemini Sigma 300 VP). The surface chemical composition of $\text{Cu}(\text{OH})_2\text{-CM}$ was analyzed by X-ray photoelectron spectroscopy (XPS, Thermo Fisher Scientific Escalab 250xl). A JY-PHB contact angle meter was applied to test the water contact angle (WCA) in air, and the underwater oil contact angle (UWOCA) on the membrane surface.

3. Results and discussion

3.1 Characterization and performance analysis

3.1.1 Surface morphology analysis with SEM

Fig. 2 shows the SEM images and optical photographs of CM, and $\text{Cu}(\text{OH})_2\text{-CM}$, illustrating the microscopic morphology changes of the mesh surface before and after treatment. From Fig. 2a, it can be seen that the untreated CM has a smooth surface without an obvious rough structure after magnification of 200 times. The pore diameter of the membrane is $45.23 \mu\text{m} - 80.64 \mu\text{m}$. Continuing to magnify to 2000 and 5000 times, Fig. 2b and c clearly show that the diameter of the individual copper wires is about $27.93 \mu\text{m}$. After oxidative treatment, the prepared $\text{Cu}(\text{OH})_2\text{-CM}$ is light blue in color (Upper right corner of Fig. 2d). The pore diameters were significantly reduced to $29.55\text{--}53.24 \mu\text{m}$. After continuing the magnification to 2000 and 5000 times, it could be observed that the surface of each copper wire was densely covered with irregular micro-nano needle-like rough structures with 3D architecture, and the diameter of the membrane filaments increased to $46.74 \mu\text{m}$ (Fig. 2e, f). Continued magnification reveals that individual micro-nano-needles have smooth surfaces with diameters of $200\text{--}300 \text{ nm}$ and lengths of $1\text{--}5 \mu\text{m}$ (Fig. 2g-i). It is this radial 3-dimensional micro-nano-needle-like rough structure that plays a crucial role in building the super-wetting surface of the mesh.

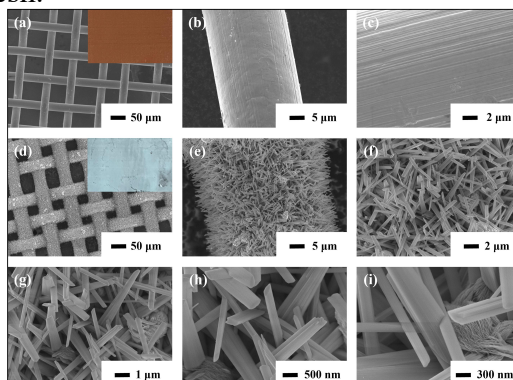


Fig. 2. SEM images and optical photographs of CM (a, b, c), $\text{Cu}(\text{OH})_2\text{-CM}$ (d, e, f, d, h, i)

3.1.2 Chemical composition analysis with XPS

It has been confirmed by SEM images that the copper mesh has been oxidized to construct a 3D rough structure on the surface, and in order to prove the hydrophilicity of this structure, the chemical composition needs to be further determined by XPS analysis, as in Fig. 3.

As shown in Fig. 3a, all the spectra were calibrated according to the C 1s photoelectron peak located at the binding energy of 284.6 eV . The full analytical energy spectrum of the surface of the calibrated copper mesh is shown in Fig. 3b, in which it can be seen that except for the photoelectron

peaks of Cu, O and C being detected, no other impurities are detected, which proves that the prepared mesh film has good purity.

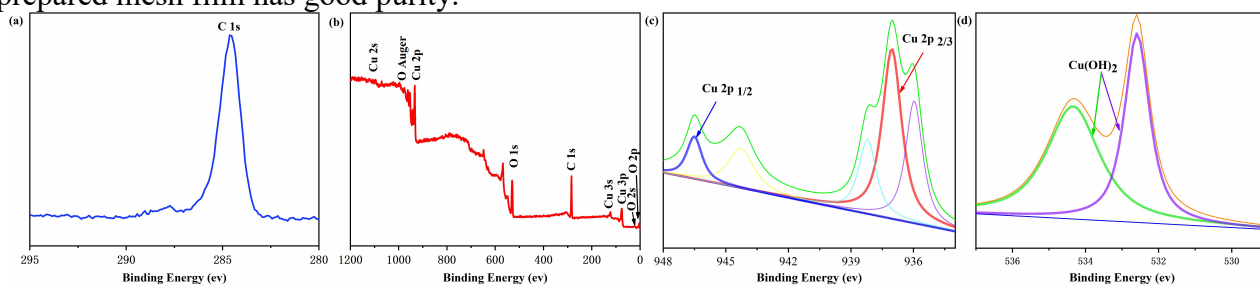


Fig. 3. XPS spectra of Cu(OH)₂-CM, XPS spectra of C 1s (a), fully analyzed XPS spectra (b), XPS spectra of Cu 2p (c) and O 1s (d) after split-peak fitting.

In order to identify the chemical valence state of the copper element, the split peaks were fitted to the Cu 2p pattern on the surface of the copper mesh samples. As shown in Fig. 3c, two photoelectron peaks of Cu 2p_{3/2} and Cu 2p_{1/2} appeared at 932.6 eV and 953.2 eV, which proved the presence of Cu²⁺ in the prepared copper mesh. According to the literature, the valence state of Cu in the samples can be determined based on the splitting width of the two Cu 2p photoelectron peaks obtained via XPS tests [10]. The two major photoelectron peaks obtained from peak splitting, 937 eV and 946.5 eV, correspond to the photoelectron peaks of Cu 2p_{2/3} and Cu 2p_{1/2}, and the width of the photoelectron peaks is about 9 eV, which further proves that the presence of Cu²⁺ [11].

The XPS spectrum of O 1s is shown in Fig. 3d, in which 532.59 eV and 534.35 eV are divided into two photoelectron peaks, and the above two photoelectron peaks can be attributed to the presence of oxygen in Cu(OH)₂. In summary, it can be proved that the mixed solution configured with potassium sulfate and sodium hydroxide reacted chemically with the copper mesh, and the radiating copper mesh surface after immersion was generated. The multi-stage rough structure on the surface of the copper mesh after immersion is copper hydroxide. The reason why the membrane acquires superhydrophilicity is that the hydroxyl groups in the copper hydroxide on the surface attracting water droplets and binding the aqueous phase through a rough structure.

3.1.3 Surface Wettability Analysis

The wettability of the material surface is closely related to oil/water separation applications, and further testing of the wettability of the membrane is essential. Fig. 4 illustrates the surface wettability of the mesh membrane at different stages of the preparation process. The untreated pure copper mesh was hydrophobic and lipophilic in air with a WCA of 112.2° (Fig. 4a). On the contrary, Cu(OH)₂-CM behaved superhydrophilic and superoleophilic in air and exhibited superoleophobicity after being wetted by water with an UWOCA of 155.4° (Fig. 4b, c). The wettability change from CM to Cu(OH)₂-CM is mainly attributed to the mesh surface's hydrophilic chemicals and rough structure. It can be understood as the hydrophilic hydroxyl groups and rough structure of the copper hydroxide can attract and trap tiny water droplets. It not only increases the contact area of the two phases, but also forms a hydrated layer on the surface of the mesh by the mass transfer to block the contact between the membrane and the oil phase, which realizes the purpose of underwater superoleophobicity.

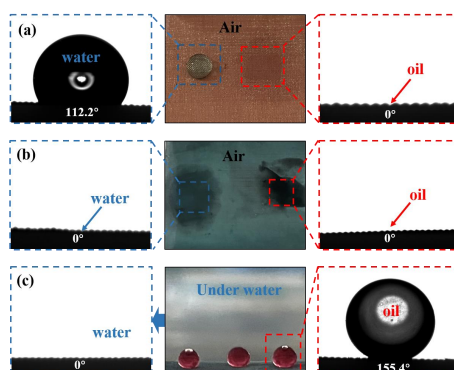


Fig. 4. Optical photographs and images of contact angles of CM (a), Cu(OH)₂-CM (b) in air and Cu(OH)₂-CM (c) underwater.

3.2 Evaluation of oil/water separation performance

To test the oil/water separation performance, we designed a simple separation device and conducted oil/water separation experiments using the gravity-driven method. As shown in Fig. 5a, Cu(OH)₂-CM was fixed in the separation device, water (30 mL) was stained with methylene blue, and test oils (hexane, 30 mL) were stained with oil red. Prior to separation, the mesh was pre-wetted with water. Due to the superhydrophilic-underwater superoleophobic property of Cu(OH)₂-CM, it can be observed that water can easily penetrate the membrane during the separation process. In contrast, n-hexane as a non-wetting phase was blocked by the membrane, which was retained above the membrane, thus achieving the selective separation of oil and water (Fig. 5b-d). Five oil phases (hexane, kerosene, xylene, diesel and gasoline) were selected to test the separation performance of the membrane. Fig. 5e shows that the separation efficiencies of Cu(OH)₂-CM for the five oil/water mixtures were all greater than 99%, and the membrane fluxes varied within the range of $3.67\text{--}6.54 \times 10^4 \text{ L} \cdot \text{m}^{-2} \cdot \text{h}^{-1}$. After repeating the oil/water separation experiments 20 times, the UWOCA of the five tested oil droplets was greater than 150° . The mesh maintained the excellent superhydrophilic-underwater superoleophobic properties, which demonstrated that the prepared Cu(OH)₂-CM not only possessed the excellent oil/water selectivity and separation efficiency, separation flux but also had good recyclability.

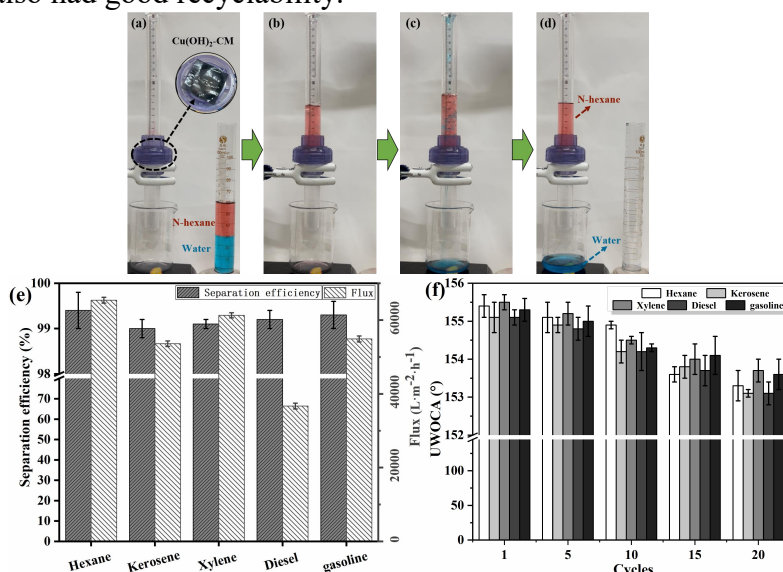


Fig. 5. The separation process of hexane using the Cu(OH)₂-CM (a-d), separation efficiency and flux for the oil/water mixture(e), The UWOCAs the Cu(OH)₂-CM after 20 times cycles(f).

3.3 Analysis of surface wettability and oil/water separation mechanism

Inspired by the wettability of lotus leaf surfaces in nature [12], rough structure and hydrophilic chemical composition are essential for constructing superhydrophilic-underwater superoleophobic surfaces. In this section, the Young and Cassie-Baxter equations are extended to the oil/water/solid three-phase system to analyze the mechanisms of mesh wettability and oil/water separation in conjunction with the CFS model.

3.3.1 Hydrophilic chemical composition

Typically, a superhydrophilic surface in the air will exhibit superoleophobic characteristics underwater [13,14]. Young's basic equation is based on the air/liquid/solid system. However, when an oil droplet is on a solid surface underwater, the extension to the oil/water/solid system can be expressed by the following equation:

$$\cos \theta_{ow} = \frac{\gamma_o \cos \theta_o - \gamma_w \cos \theta_w}{\gamma_{ow}} \quad (3)$$

where γ_o , γ_w and γ_{ow} represent the interfacial tensions of oil/air, water/air and oil/water, respectively, and θ_o , θ_w and θ_{ow} represent the contact angles of oil in air, water in air and oil in water, respectively.

From equation (3), if the solid surface is hydrophilic ($\theta_w < 90^\circ$), since the surface tension of oil in air γ_o is considerably lower than the surface tension of water in air γ_w , it means that this solid surface is oleophilic ($\theta_o < 90^\circ$), and $\cos \theta_o$ and $\cos \theta_w$ are both positive, so the value of $\gamma_o \cos \theta_o - \gamma_w \cos \theta_w$ is usually negative, and γ_{ow} is positive, and $\cos \theta_{ow}$ is negative, i.e., $\theta_{ow} > 90^\circ$, which means that the surface that presents hydrophilic and oleophilic properties in this air can realize the nature of the underwater oleophobicity [15].

3.3.2 Rough structure

Extension of Cassie's equation from the water/gas/solid three-phase system to the oil/water/solid three-phase system can further explain the underwater superoleophobic behavior of the mesh.

$$\cos \theta_3' = f \cos \theta_3 + f - 1 \quad (4)$$

Where f is the area fraction of the oil-solid interface, θ_3 is the UWOCA on a smooth solid surface, and θ_3' is the UWOCA on the surface of Cu(OH)₂-CM. A decrease in f leads to an increase in θ_3' , i.e., a decrease in the area of the oil droplet in contact with the solid or an increase in the area of the aqueous phase in contact with the solid causes an increase in the apparent underwater oil contact angle. The oil/solid interfacial fractions of the five oil samples on the surface of the Cu(OH)₂-CM were calculated by substituting the experimentally measured θ_3 , θ_3' , into Eq. (4), and the data are shown in Table 1.

Table 1. Fraction of area of the Cu(OH)₂-CM in contact with the oil phase in the oil/water/solid system.

Oil	$\theta_3(^{\circ})$	$\theta_3'(^{\circ})$	$f(\%)$
Hexane	66.5	155.4	6.49
Kerosene	67.3	155.1	6.71
Xylene	65.6	155.5	6.37
Diesel	67.2	155.1	6.70
gasoline	68.1	155.3	6.67

Table 1 shows the theoretical contact area between Cu(OH)₂-CM and oil droplets in the aqueous phase environment. From the table, the contact area between the five tested oil phases and the surface of the mesh is less than 6.71%, which indicates that surfaces with micro and nano-scale roughness structures can capture small molecules of the wetting phase, and the larger the roughness is, the greater the ability to bind the small molecules of the wetting phase is. The wetting phase forms a layer of liquid on the surface of the mesh, which significantly reduces the contact with the non wetting phase, thus achieving the effect of the more roughness, the more oleophobic.

For the Cu(OH)₂-CM prepared using copper mesh as the substrate, the SEM image Fig. 2e shows that the membrane filaments have a cylindrical-like geometry and a physical model can be introduced to further reveal the wetting behaviour of the mesh surface. The space between two neighbouring membrane filaments can be regarded as a capillary model (CFS model), and the wetting behaviour of the liquid phase in this model can be revealed through the capillary phenomenon. Penetration pressure (ΔP_c) is an important physical property for evaluating the efficiency of oil/water separation in mesh [12]. Fig. 6 shows the cross-sectional force model of the oil/water phase on two neighbouring membrane filaments on the mesh surface.

The penetration pressure (ΔP_c) is the maximum pressure exerted on the surface before the liquid penetrates the membrane pores, and ΔP_c was calculated according to the Young-Laplace equation [16] (5):

$$\Delta P_c = -\frac{2\gamma_L \cos \theta}{r_p} \quad (5)$$

Where γ_L is the surface tension of the liquid phase, θ is the contact angle of the liquid phase on the surface of the material, and r_p is the radius of the membrane pore, evidently the wettability of the surface has a significant effect on the penetration pressure. As shown in Fig. 6a, in air, the surface of the $\text{Cu}(\text{OH})_2\text{-CM}$ constitutes a three-phase interface with the air and water phases, which exhibits superhydrophilicity. At this time, $\theta < 90^\circ$, $\Delta P_c < 0$, the surface of the mesh is unable to withstand the pressure exerted by the water phase, and it exhibits the capillary effect in the three-phase system of water/gas/solid, suggesting that the water phase can spontaneously penetrate and wet the mesh entirely without any external additional pressure.

$$\Delta P_c^w = -\frac{2\gamma_{ow} \cos \theta_{ow}}{r_p} \quad (6)$$

When the surface of the mesh is wetted by the aqueous phase and comes into contact with the oil phase, it can be explained by Equation 6. In the formula, θ_{ow} is the contact angle of underwater oil droplets, γ_{ow} is the oil/water interfacial tension, and r_p is the radius of membrane pores. The mesh exhibits underwater superoleophobic properties in the oil/water/solid three-phase system. As shown in Fig. 6b, in the aqueous environment, the contact angle of oil droplets on the surface of the mesh $\theta_{ow} > 90^\circ$, and the derivation of Eqs.6 shows that $\Delta P_c^w > 0$, which indicates that it is necessary to apply additional pressure to make the oil phase through the mesh. Usually, for separating the oil/water mixtures, the closer the mesh's WCA is to 0° in air, and the closer the UWOCA is to 180° . It means that it is more hydrophilic the more oleophobic it is under the water, the greater the upward penetration pressure for the oil phase and the downward penetration pressure for the aqueous phase is, the better the selective separation of the two phases is. The more the mesh makes it possible for the oil phase to pass through.

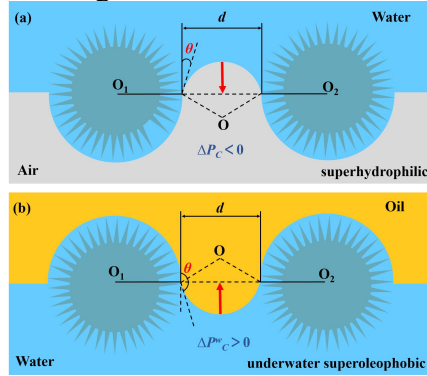


Fig. 6. Schematic diagram of liquid force on the surface of the $\text{Cu}(\text{OH})_2\text{-CM}$

4. Summary

Superhydrophilic-submerged superoleophobic $\text{Cu}(\text{OH})_2\text{-CM}$ were successfully prepared by an in situ growth method. The super-wetted surface of the mesh was densely covered with micro and nanoscale needle-like rough structures of three dimensional architecture, and the gravity-driven separation efficiency of the membrane for the five tested oils was maintained at more than 99%, with a separation flux of up to $6.54 \times 10^4 \text{ L} \cdot \text{m}^{-2} \cdot \text{h}^{-1}$. The excellent wetting characteristics of the membrane were still maintained after performing 20 repetitions of the experiments. The surface wettability and oil/water separation mechanism were analyzed in detail by the CFS model combined with Young and Cassie-Baxter equations. The next step is to discuss the relationship between the separation flux and the penetration pressure, membrane thickness and membrane pore size using the Hagen-Poiseuille equation. Considering the practical application environment of $\text{Cu}(\text{OH})_2\text{-CM}$, the

separation performance in extreme environments (seawater, different UV irradiation, solutions with different pH values and temperatures) will be explored in the future.

References

- [1] ZHENG W, HUANG J, LI S, et al. Advanced Materials with Special Wettability toward Intelligent Oily Wastewater Remediation[J]. *ACS Applied Materials & Interfaces*, 2021, 13(1): 67-87.
- [2] YALCINKAYA F, BOYRAZ E, MARYSKA J, et al. A Review on Membrane Technology and Chemical Surface Modification for the Oily Wastewater Treatment[J]. *Materials*, 2020, 13(2): 493.
- [3] FENG L, LI S, LI Y, et al. Super-Hydrophobic Surfaces: From Natural to Artificial[J]. *ChemInform*, 2003, 34(7): 1857-1860.
- [4] YONG J, YANG Q, HOU X, et al. Emerging Separation Applications of Surface Superwettability[J]. *Nanomaterials*, 2022, 12(4): 688.
- [5] PADAKI M, SURYA MURALI R, ABDULLAH M S, et al. Membrane technology enhancement in oil–water separation. A review[J]. *Desalination*, 2015, 357: 197-207.
- [6] BAIG U, FAIZAN M, DASTAGEER M A. Polyimide based super-wettable membranes/materials for high performance oil/water mixture and emulsion separation: A review[J]. *Advances in Colloid and Interface Science*, 2021, 297: 102525.
- [7] WEI Y, QI H, GONG X, et al. Specially Wettable Membranes for Oil–Water Separation[J]. *Advanced Materials Interfaces*, 2018, 5(23): 1800576.
- [8] XUE Z, WANG S, LIN L, et al. A Novel Superhydrophilic and Underwater Superoleophobic Hydrogel-Coated Mesh for Oil/Water Separation[J]. *Advanced Materials*, 2011, 23(37): 4270-4273.
- [9] GAO X, XU L P, XUE Z, et al. Dual-Scaled Porous Nitrocellulose Membranes with Underwater Superoleophobicity for Highly Efficient Oil/Water Separation[J]. *Advanced Materials*, 2014, 26(11): 1771-1775.
- [10] VASQUEZ R P. Cu(OH)₂ by XPS[J]. *Surface Science Spectra*, 1998, 5(4): 267-272.
- [11] XU G, DENG L, WEN X, et al. Synthesis and characterization of fluorine-containing poly-styrene-acrylate latex with core–shell structure using a reactive surfactant[J]. *Journal of Coatings Technology and Research*, 2011, 8(3): 401-407.
- [12] CHEN C, WENG D, MAHMOOD A, et al. Separation Mechanism and Construction of Surfaces with Special Wettability for Oil/Water Separation[J]. *ACS applied materials & interfaces*, 2019, 11(11): 11006-11027.
- [13] XUE Z, CAO Y, LIU N, et al. Special wettable materials for oil/water separation[J]. *J. Mater. Chem. A*, 2014, 2(8): 2445-2460.
- [14] XUE Z, LIU M, JIANG L. Recent developments in polymeric superoleophobic surfaces[J]. *Journal of Polymer Science Part B: Polymer Physics*, 2012, 50(17): 1209-1224.
- [15] YANG J, GAO M, SUN H, et al. Simulation of the dynamic behavior of droplet impact on the microstructure surface[J]. *Journal of Physics: Conference Series*, 2023, 2441(1): 012064.
- [16] KIM B S, HARRIOTT P. Critical entry pressure for liquids in hydrophobic membranes[J]. *Journal of Colloid and Interface Science*, 1987, 115(1): 1-8.